

Measurement of the neutron capture cross section of ^{236}U

F. Gunsing^{*1}, P. Schillebeeckx², R. Wynants², S. Andriamonje¹, E. Berthoumieux¹,
A. Borella¹, W. Dridi¹, W. Furman³, A. Goverdovski⁴, C. Lampoudis^{5,1},
H. Álvarez⁶, U. Abbondanno⁷, G. Aerts¹, F. Alvarez-Velarde⁸, J. Andrzejewski⁹,
P. Assimakopoulos¹⁰, L. Audouin¹¹, G. Badurek¹², P. Baumann¹³, F. Bečvář¹⁴,
F. Calviño¹⁵, D. Cano-Ott⁸, R. Capote^{16,17}, A. Carrillo de Albornoz¹⁸, P. Cennini¹⁹,
V. Chepel²⁰, E. Chiaveri¹⁹, N. Colonna²¹, G. Cortes²², A. Couture²³,
J. Cox²³, M. Dahlfors¹⁹, S. David¹¹, I. Dillman²⁴, R. Dolfini²⁵, C. Domingo-Pardo²⁶,
I. Duran⁶, C. Eleftheriadis⁵, M. Embid-Segura⁸, L. Ferrant¹¹, A. Ferrari¹⁹, R. Ferreira-Marques²⁰,
H. Frais-Koelbl¹⁶, K. Fujii⁷, I. Goncalves²⁰, E. Gonzalez-Romero⁸, F. Gramegna²⁷, E. Griesmayer¹⁶,
C. Guerrero⁸, B. Haas²⁸, R. Haight²⁹, M. Heil²⁴, A. Herrera-Martinez¹⁹, M. Igashira³⁰,
S. Isaev¹¹, E. Jericha¹², F. Käppeler²⁴, Y. Kadi¹⁹, D. Karadimos¹⁰, D. Karamanis¹⁰,
M. Kerveno¹³, V. Ketlerov^{4,19}, P. Koehler³¹, V. Konovalov^{3,19}, E. Kossionides³²,
M. Krčička¹⁴, H. Leeb¹², A. Lindote²⁰, I. Lopes²⁰, M. Lozano¹⁷, S. Lukic¹³,
J. Marganec⁹, L. Marques¹⁸, S. Marrone²¹, C. Massimi³³, P. Mastinu²⁷, A. Mengoni^{16,19},
P.M. Milazzo⁷, C. Moreau⁷, M. Mosconi²⁴, F. Neves²⁰, H. Oberhummer¹², S. O'Brien²³,
M. Oshima³⁴, J. Pancin¹, C. Papachristodoulou¹⁰, C. Papadopoulos³⁵, C. Paradela⁶, N. Patronis¹⁰,
A. Pavlik³⁶, P. Pavlopoulos³⁷, L. Perrot¹, M.T. Pigni¹², R. Plag²⁴, A. Plompen²,
A. Plukis¹, A. Poch²², C. Pretel²², J. Quesada¹⁷, T. Rauscher³⁸, R. Reifarh²⁹,
M. Rosetti³⁹, C. Rubbia²⁵, G. Rudolf¹³, P. Rullhusen², J. Salgado¹⁸, L. Sarchiapone¹⁹,
I. Savvidis⁵, C. Stephan¹¹, G. Tagliente²¹, J.L. Tain²⁶, L. Tassan-Got¹¹, L. Tavora¹⁸,
R. Terlizzi²¹, G. Vannini³³, P. Vaz¹⁸, A. Ventura³⁹, D. Villamarin⁸, M.C. Vincente⁸,
V. Vlachoudis¹⁹, R. Vlastou³⁵, F. Voss²⁴, S. Walter²⁴, H. Wendler¹⁹,
M. Wiescher²³, K. Wisshak²⁴

The n_TOF Collaboration

¹CEA/Saclay - DSM/DAPNIA, Gif-sur-Yvette, France

²CEC-JRC-IRMM, Geel, Belgium

³Joint Institute for Nuclear Research, Frank Laboratory of Neutron Physics, Dubna, Russia

⁴Institute of Physics and Power Engineering, Kaluga region, Obninsk, Russia

⁵Aristotle University of Thessaloniki, Greece

⁶Universidad de Santiago de Compostela, Spain

⁷Istituto Nazionale di Fisica Nucleare, Trieste, Italy

⁸Centro de Investigaciones Energeticas Medioambientales y Tecnologicas, Madrid, Spain

⁹University of Lodz, Lodz, Poland

¹⁰University of Ioannina, Greece

¹¹Centre National de la Recherche Scientifique/IN2P3 - IPN, Orsay, France

¹²Atominstut der Österreichischen Universitäten, Technische Universität Wien, Austria

¹³Centre National de la Recherche Scientifique/IN2P3 - IReS, Strasbourg, France

¹⁴Charles University, Prague, Czech Republic

¹⁵Universidad Politecnica de Madrid, Spain

¹⁶International Atomic Energy Agency (IAEA), Nuclear Data Section, Vienna, Austria

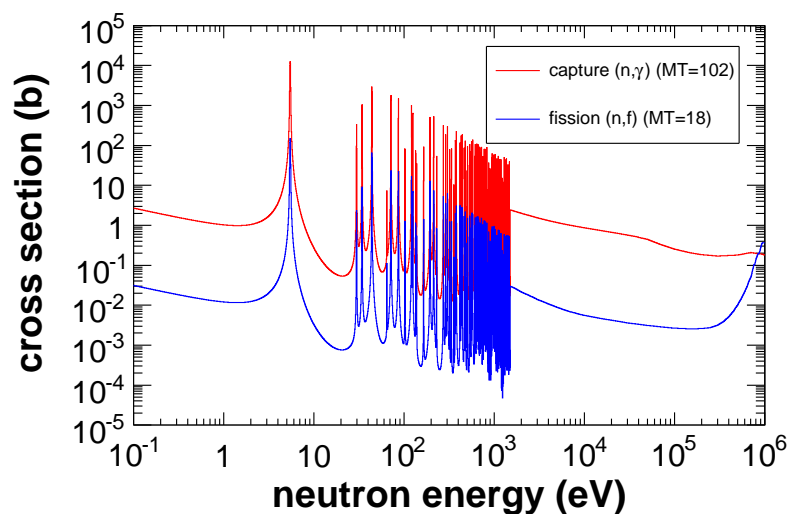
- ¹⁷Universidad de Sevilla, Spain
¹⁸Instituto Tecnológico e Nuclear(ITN), Lisbon, Portugal
¹⁹CERN, Geneva, Switzerland
²⁰LIP - Coimbra & Departamento de Física da Universidade de Coimbra, Portugal
²¹Istituto Nazionale di Fisica Nucleare, Bari, Italy
²²Universitat Politècnica de Catalunya, Barcelona, Spain
²³University of Notre Dame, Notre Dame, USA
²⁴Forschungszentrum Karlsruhe GmbH (FZK), Institut für Kernphysik, Germany
²⁵Università degli Studi Pavia, Pavia, Italy
²⁶Instituto de Física Corpuscular, CSIC-Universidad de Valencia, Spain
²⁷Istituto Nazionale di Fisica Nucleare(INFN), Laboratori Nazionali di Legnaro, Italy
²⁸Centre National de la Recherche Scientifique/IN2P3 - CENBG, Bordeaux, France
²⁹Los Alamos National Laboratory, New Mexico, USA
³⁰Tokyo Institute of Technology, Tokyo, Japan
³¹Oak Ridge National Laboratory, Physics Division, Oak Ridge, USA
³²NCSR, Athens, Greece
³³Dipartimento di Fisica, Università di Bologna, and Sezione INFN di Bologna, Italy
³⁴Japan Atomic Energy Research Institute, Tokai-mura, Japan
³⁵National Technical University of Athens, Greece
³⁶Institut für Isotopenforschung und Kernphysik, Universität Wien, Austria
³⁷Pôle Universitaire Léonard de Vinci, Paris La Défense, France
³⁸Department of Physics and Astronomy - University of Basel, Basel, Switzerland
³⁹ENEA, Bologna, Italy

Abstract

In this paper we describe the $^{236}\text{U}(n,\gamma)$ reaction cross section measurement at the GELINA white pulsed neutron source of the Institute for Reference Materials and Measurements (IRMM) in Geel. The sample was placed in the neutron beam at a flight station located at a nominal distance of 30 m from the neutron source. Neutron capture gamma rays were detected by two C_6D_6 -based liquid scintillator gamma-ray detectors as a function of the neutron time-of-flight using the pulse height weighting technique. The pulse height weighting function has been derived from Monte Carlo simulations of the detector response to mono-energetic gamma rays. The shape of the neutron flux was measured with a ^{10}B chamber, placed about 60 cm upstream in the neutron beam. The capture yield in the resolved resonance region up to 3 keV has been derived and will be presented here. The analysis of the capture yield in terms of R -matrix resonance parameters is planned for the near future.

KEYWORDS: *neutron capture, measurement, time of flight, GELINA, resonances, ^{236}U*

*corresponding author: F. Gunsing, gunsing@cea.fr

Figure 1: The JEFF3.1 evaluation for the ^{236}U neutron capture and fission cross section.

1. Introduction

The accurate knowledge of neutron-induced reaction cross sections is important for applications in nuclear technology. In the past much emphasis has been put on the measurement and evaluation of nuclear data for the existing generation of nuclear power plants. New applications, like the high burn-up of current fuels, Generation IV reactors, alternative fuel cycles, transmutation of nuclear waste or accelerator driven systems, address other isotopes, energy ranges and reactions for which improved nuclear data are mandatory. The capture cross section of ^{236}U is particularly important for the build-up of higher actinides in nuclear fuel, both in the uranium-based fuel cycle, where ^{236}U is produced by capture on ^{235}U , as in the possible future fuel cycle based on ^{232}Th .

The evaluations of the $^{236}\text{U}(n,\gamma)$ cross section in the resolved resonance region from the evaluated nuclear data libraries are based on a small number of existing measurements. The capture cross section was measured by Carlson *et al.* [1], and later by Mewissen *et al.* [2], who also measured scattering and transmission. An early transmission experiment was done by Harvey and Hughes [3]. Another transmission experiment was reported by Carraro and Brusegan [4]. Also Macklin and Alexander measured neutron transmission on ^{236}U [5].

The fission cross section has been investigated [6–8] as well. The particular interest for the isotope ^{236}U arises from the intermediate structure in the fission cross section. This structure is related to the double-humped fission barrier. Eigenstates corresponding to the secondary potential well in the fission barrier, also called class-II states, have much larger fission probabilities than the usual class-I states in the primary well. The class-II states are also more widely spaced, even up to a hundred times larger than the class-I states. This results in clusters of resonances with a strong fission cross section and is common for many actinides. Several of these intermediate structure resonances have been found for actinides, like ^{237}Np , and the even-mass uranium and plutonium isotopes.

A high fission strength in several resonance groups has been observed by Parker *et al.* [8]. The first cluster is situated rather high, around 1281 eV, and has a high fission width larger than

expected from calculations. A recent fission measurement has confirmed this observation [9]. Note that these strong resonances are not present in the evaluated libraries of ^{236}U , as can also be seen in figure 1.

A closer investigation of the capture cross section in this region may exclude any anomalous contribution from capture to the fission experiments. We have undertaken this neutron capture experiment on ^{236}U within the scientific program of the n_TOF collaboration.

2. Experimental setup

The capture cross section measurement on ^{236}U was performed using the time-of-flight technique at the pulsed neutron facility GELINA of the Joint Research Centre IRMM in Geel, Belgium. This facility with its linear electron accelerator and its neutron producing target has previously been described in detail [10–12]. The Linac has been operating to provide electron bursts of 100 MeV average energy and 1 ns width at a repetition rate of 800 Hz and an average beam current of $70\ \mu\text{A}$.

Neutrons were produced by (γ, n) and (γ, f) reactions, induced via Bremsstrahlung from the electron beam hitting a rotating, mercury cooled uranium target. The neutron spectrum from the target was moderated by water contained in a 4 cm thick beryllium casing, situated beneath and above the target. The partially thermalized neutrons scattered from the moderators were collimated into the flight path through evacuated aluminum pipes of 50 cm diameter with collimators consisting of borated wax, copper and lead, placed at regular distances. A shadow bar made of copper and lead was placed in front of the uranium target, in this way preventing fast neutrons from the rotary target to go into the flight paths. In addition the shadow bar attenuated the intense burst of gamma rays created immediately after the impact of the electrons on the target. The neutron intensity was continuously monitored by BF_3 detectors located at different positions around the target hall.

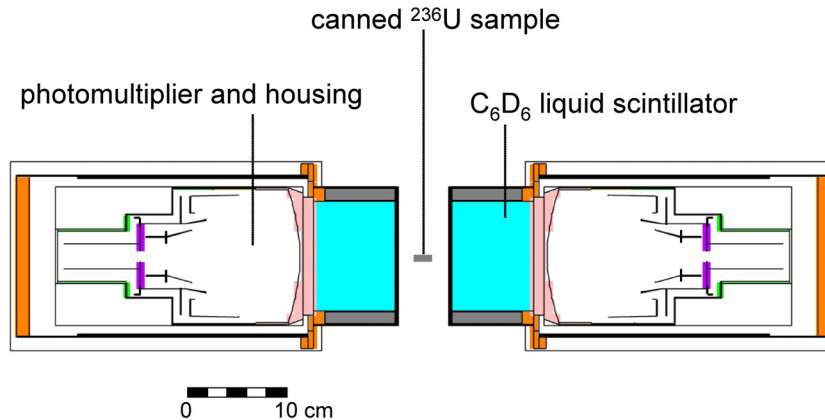
We have used the neutron beam line making an angle of -90° with respect to the electron beam. The sample was placed in the neutron beam at the flight station located at 28.6 m from the neutron production target.

In order to absorb slow neutrons that otherwise overlap with the next machine cycle, a cut-off filter of $^{10}\text{B}_4\text{C}$ with a thickness of 0.013 at/b of ^{10}B was placed in the neutron beam, about 20 m upstream of the sample position. Since with this thickness of ^{10}B the neutron flux is rather low for the first few resonances, we also performed a measurement with a 0.004 at/b thick $^{\text{nat}}\text{Cd}$ anti-overlap filter instead of ^{10}B . Since Cd has many resonances affecting the shape of the neutron flux, we used this data only for the first few resonances. At the same location additional neutron filters of Ag, W, Co, Na and S with appropriate thicknesses were placed in the beam during dedicated background measurements.

A sample with a total amount of 338 mg of ^{236}U has been prepared by the Institute of Physics

Table 1: Isotopic composition of the ^{236}U sample in mass percent.

nucleus	(wt. %)
^{235}U	0.05
^{236}U	99.85
^{238}U	0.10

Figure 2: A schematic view of the detector-sample configuration of the neutron capture setup.

and Power Engineering (IPPE) in Obninsk. Enriched uranium oxide $^{236}\text{U}_3\text{O}_8$ was pressed into a pellet of 10 mm diameter and placed inside a ring of 0.25 mm thick high purity aluminum with 10 mm inner and 15 mm outer diameter. We have used high purity aluminum in order to avoid neutron capture on the nuclei from additions like manganese, present in standard aluminum. On both sides of the ring containing the uranium sample, a 0.25 mm thick high purity aluminum disk with 15 mm diameter was glued. In this way the sample was sealed for practical purposes, while still having a low mass canning, essential for capture measurements. The results of an isotopic analysis performed at IPPE is shown in table 1.

Two hydrogen-free, C_6D_6 -based liquid scintillator gamma-ray detectors (NE230), each coupled through a boron-free quartz window to a EMI9823 KQB photomultiplier, were placed out of the neutron beam at the sample position, with a distance of 50 mm between them.

To measure the relative neutron flux, we installed in the beam about 60 cm upstream of the sample a neutron flux detector, consisting of a boron ionization chamber with a $40 \mu\text{g}/\text{cm}^2$ deposit of ^{10}B on both sides of the cathode in a continuous flow of a gas composed of 90% argon and 10% methane.

Because of the small amount of sample material, the sample diameter was only 10 mm. The detectors were also placed close to the sample to optimize the count rate. We therefore adapted the collimation at about 1.5 m upstream of the sample position in order to have a neutron beam with a diameter slightly larger than the sample diameter. The usual beam diameter is typically 80 mm. Therefore also the flux measurements have been done with the small beam diameter, reducing largely the count rate in the boron ionization chamber.

The amplitude and time-of-flight information was extracted from the detector signals by respectively Canberra 8715 ADCs and a 25 bit in-house developed [13] multi-hit time digitizer with 0.5 ns resolution. In order to minimize the dead time, the events from the capture detectors and from the boron ionization chamber were taken by two independent data acquisition systems. The dead time for the flux measurement was $3.1 \mu\text{s}$ and for the capture measurement $3.8 \mu\text{s}$. A fixed dead time correction was applied to all raw counting spectra.

For the experiment, a total amount of effective beam time of more than 800 hours was used for data taking, including background measurements. The detector events and associated information were written on disk for off-line analysis.

3. Data reduction

3.1 Weighting function

The signature of a (n,γ) reaction is the gamma cascade de-exciting the compound nucleus in the capture state. In order to make the detection efficiency of a capture event independent from the decay cascade, one usually applies the pulse height weighting technique (PHWT) [14–17] if the detection system does not have 100% efficiency and does not cover a 4π solid angle. The PHWT consists of making artificially the detector's efficiency ϵ_γ proportional to the incident gamma-ray energy E_γ by applying a weighting function $W(E_d)$ such that

$$\epsilon_\gamma = \int W(E_d)R_\gamma(E_d)dE_d = kE_\gamma \quad (1)$$

where $R_\gamma(E_d)$ is the detector's response as a function of the deposited energy E_d . The weighting function $W(E_d)$ has been derived using Monte Carlo simulations with the code MCNP [18] of the detector response $R_\gamma(E_d)$ to different mono-energetic gamma rays and solving equation 1 by minimization. A 4th order polynomial was sufficient to describe the weighting function $W(E_d)$. Then the weighted count rate spectrum $C_W(E_n)$ can be written as

$$C_W(E_n) = \int R_\gamma(E_d)W(E_d)dE_d = \Phi(E_n)Y(E_n)E_c \quad (2)$$

where $\Phi(E_n)$ is the energy distribution of the number of neutrons incident on the sample and E_c is the cascade energy or excitation energy of the compound nucleus.

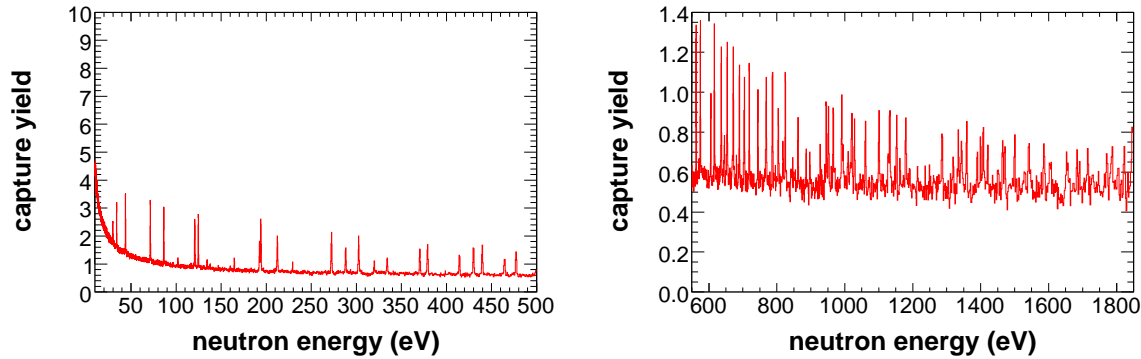
The pulse height distribution of the C_6D_6 detectors was calibrated in energy using the detector response of the radioactive sources ^{137}Cs , ^{60}Co and a composite source of the alpha-emitter ^{238}Pu and carbon, giving a 6.13 MeV gamma-ray through the $^{13}C(\alpha, n)^{16}O^*$ reaction. A simultaneous fit matching the three measured responses to simulated energy deposits results in a nearly linear energy calibration in the range from the threshold energy of 150 keV deposited energy to about 6 MeV, largely above the neutron separation energy of ^{237}U at 5.126 MeV.

3.2 Determination of the neutron flux

The time-of-flight spectra for the flux measurements were constructed from the events with an amplitude within a window corresponding to the energy deposit of the α and 7Li particles from the $^{10}B(n,\alpha)^7Li$ reaction. The background in the boron ionization chamber originates from the residual scattered and thermalized neutrons present in the experimental area and from neutrons from previous cycles that are not stopped by the anti-overlap filter.

The shape of the background on the flux measurement was estimated by placing neutron filters in the beam. These filters consisted of foils or encapsulated material with nuclei showing large resonances at specific energies, removing all neutrons from the beam at these energies. The remaining detected counts at the black resonance energies, showing an amplitude spectrum corresponding to detected neutrons, come from background neutrons not having the time-energy correlation. Filters of Ag, W, Co, Na and S were used to determine the shape of the background, that could be modelled as a function of time of flight t by the simple form $B_\Phi(t) = a_1 + a_2t^{a_3}$, with $B_\Phi(t)$ the number of counts per unit time of flight.

This background shape was then subtracted from the flux measurement $\Phi(t)$ without the filters except one. The absolute level of the background was determined with this permanent filter, either sodium with a black resonance at 2.8 keV, or sulfur with a black resonance at 102.71 and 112.18 keV.

Figure 3: Part of the unnormalized neutron capture yield of ^{236}U .

3.3 Capture yield

The experimental capture yield $Y(E_n)$ was then extracted from the measured spectra as

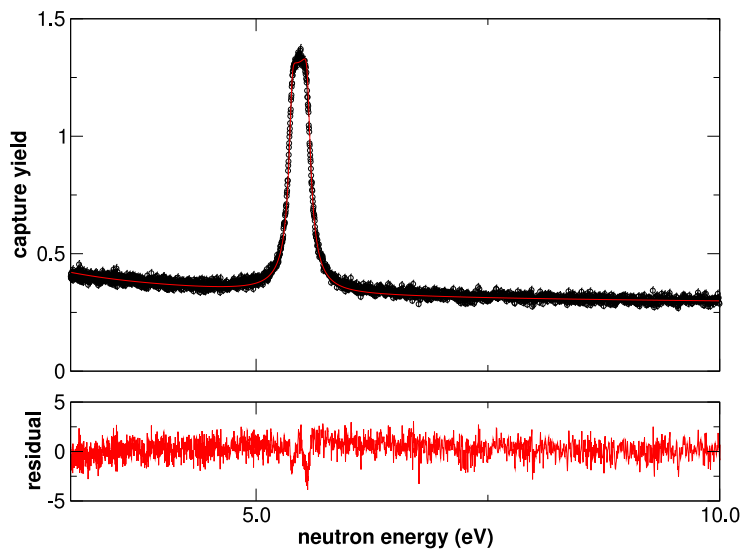
$$Y(E_n) = N \times \frac{C_W(E_n)/E_c}{\Phi(E_n) - B_\Phi(E_n)} \quad (3)$$

It should be noted that this yield still contains the background measured with the C_6D_6 detectors. This background consists mainly of the radioactivity of the decay products of the sample and ambient radioactivity, and is constant per unit of time. Neutrons scattered from the sample and subsequently captured in the surrounding materials also contribute to the background. This background follows the resonance structure of the scattering cross section of the target nucleus and depends on two factors, the neutron sensitivity and the scattering to capture ratio of the target nucleus. The detector itself and its environment determine the neutron sensitivity which should be optimized to be as low as possible and which should be measured or modelled to be taken into account. Typically C_6D_6 detectors have a very low neutron sensitivity. A large scattering to capture ratio of the target nucleus results in a larger background from sample scattered neutrons. This is in particular the case for light or near-magic nuclei where the scattering cross section may be more than a factor 1000 larger than the capture cross section. For difficult situations also the detector canning can be optimized [19] with respect to commercially available detectors. For the present case of ^{236}U this background component is low.

The capture yield was normalized to the first s -wave resonance of $^{236}\text{U}+n$ at 5.45 eV. This resonance is not visible with the measurements using the ^{10}B anti-overlap filter because of the nearly zero neutron flux at that energy. For this purpose we used the measurement with the Cd anti-overlap filter. A fit of this resonance with the code SAMMY [20] is shown in figure 4.

The capture yield is shown in figure 3. The left panel of the figure shows the energy range from 0 to 500 eV. One can see the radioactive background at low energy where the energy bins correspond to large time intervals. The first resonance is not visible in this spectrum. The right panel of figure 3 shows the capture yield in a large energy range around 1281 eV. From the figure it can be seen that no anomalous capture yield is observed. Therefore it seems unlikely that the large fission width for the 1281 eV resonance observed in the measurements from Cramer and Bergen [6] and Parker *et al.* [8] suffered from an experimental effect related to capture.

Figure 4: The first s -wave resonance of ^{236}U . The capture yield is saturated allowing to determine the normalization.



4. Conclusion

A new measurement of the $^{236}\text{U}(n,\gamma)$ neutron capture cross section in the resonance region has been performed at the GELINA white pulsed neutron source. Data have been taken with a low mass sample containing 338 mg ^{236}U and have been transformed in an experimental capture yield and the analysis of the resolved resonances is ongoing. A simultaneous resonance analysis of available capture, fission and also transmission experiments is recommended in order to obtain a reliable set of resonance parameters.

Acknowledgements

This work has been supported by the European Commission's 5th Framework Programme under contract number FIKW-CT-2000-00107 (n-TOF-ND-ADS Project).

References

- 1) A. D. Carlson, S. H. Friesenhahn, W. M. Lopez, and M. P. Fricke, "The ^{236}U neutron capture cross section", *Nucl. Phys.* **A141** 577 (1970)
- 2) L. Mewissen, F. Poortmans, G. Rohr, J. P. Theobald, H. Weigmann, and G. Vanpraet, "Neutron cross-section measurement on ^{236}U ", In R. A. Schrack and C. D. Bowman, editors, *Proc. Conf. Nuclear Cross Sections and Technology*, Washington D.C., 729, (1975)
- 3) J. A. Harvey and D. J. Hughes, "Spacings of Nuclear Energy Levels", *Phys. Rev.* **109** 471 (1958)
- 4) G. Carraro and A. Brusegan, "Total neutron cross section measurements of ^{236}U in the energy range 40 eV to 4.1 keV", *Nucl. Phys.* **A257** 333 (1976)

- 5) R. L. Macklin and C. W. Alexander, "Neutron absorption cross section of ^{236}U ", *Nucl. Sci. Eng.* **104** 258 (1990)
- 6) J. D. Cramer and D. W. Bergen, Los Alamos Report No. LA-4420, 74 (1970)
- 7) J. P. Theobald, J. A. Wartena, and H. Weigmann, "Fission components in ^{236}U neutron resonances", *Nucl. Phys.* **A181** 639 (1972)
- 8) W. E. Parker, E. Lynn, G. L. Morgan, P. W. Lisowski, A. D. Carlson, and N. W. Hill, "Intermediate structure in the neutron-induced fission cross section of ^{236}U ", *Phys. Rev. C* **49** 672 (1994)
- 9) W. Furman *et al.* (the n_TOF Collaboration), unpublished.
- 10) D. Tronc, J. M. Salomé and K. H. Böckhoff, *Nucl. Instrum. Methods Phys. Res. A* **228** 217 (1985)
- 11) J. M. Salomé, *Physicalia* **8** 261 (1986)
- 12) M. Flaska, A. Borella, D. Lathouwers, L. C. Mihailescu, W. Mondelaers, A. J. M. Plompen, H. van Dam, and T. H. J. J. van der Hagen, "Modeling of the GELINA neutron target using coupled electron-photon-neutron transport with the MCNP4C3 code". *Nucl. Instrum. Methods Phys. Res. A* **531** 392 (2004)
- 13) S. de Jonge, "Fast Time Digitizer Type 8514 A, Internal Report GE/DE/R/24/87, IRMM, Geel (1987)
- 14) R. L. Macklin and J. H. Gibbons, "Capture-Cross-Section Studies for 30-220 keV Neutrons Using a New Technique", *Phys. Rev* **159** 1007 (1967)
- 15) F. Corvi *et al.* , "The weighting function of a neutron capture detection system", *Nucl. Sci. Eng.* **107** 272 (1991)
- 16) J. N. Wilson, B. Haas, S. Boyer, D. Dassié, G. Barreau, M. Aiche, S. Czajkowski, C. Grosjean, and A. Guiral, "Measurements of (n, γ) neutron capture cross-sections with liquid scintillator detectors", *Nucl. Instrum. Methods Phys. Res. A* **511** 388 (2003)
- 17) U. Abbondanno *et al.* , "New experimental validation of the pulse height weighting technique for capture cross-section measurements", *Nucl. Instrum. Methods Phys. Res. A* **521** 454 (2004)
- 18) J. F. Briesmeister, Ed., *MCNP - A General Monte Carlo N-Particle Transport Code, Version 4C*, LA-13709-M (2000), version 4C3
- 19) R. Plag *et al.* "An optimized C_6D_6 detector for studies of resonance-dominated (n, γ) cross-sections", *Nucl. Instrum. Methods Phys. Res. A* **496** 425 (2003)
- 20) N. M. Larson, "Updated users' guide for SAMMY: Multilevel R-matrix fits to neutron data using Bayes' equations" SAMMY, computer code Report ORNL/TM-9179/R7, Oak Ridge National Laboratory (2006)